

Retrieval of Surface Solar Radiation Budget: Corrections for Ice Clouds

Y. Zhang and Z. Li
EMS, Canada Centre for Remote Sensing
Ottawa, K1A 0Y7, Canada

A. Macke
Institut fuer Meereskunde
24105 Kiel, Germany

Introduction

Surface solar radiative budget (SSRB) is modulated primarily by clouds whose effects must be taken into account carefully in estimating it from satellite measured upward solar radiative flux at top of the atmosphere (TOA). To avoid time-consuming calculations in operational retrieval of SSRB from satellite, Li et al. (1993) derived a simple linear parameterization scheme based on the results of radiative transfer simulation. They found that, for more than 90% of clear- and cloudy-sky cases, estimated SSRB using the linear relationship has an error within 10 Wm^{-2} of model simulations. Errors larger than 20 Wm^{-2} corresponded cloud cases, especially for ice clouds. Masuda et al. (1995) introduced corrections to better account for the effects of water clouds, ground surface pressure, ozone amount, aerosol type, cloud effective droplet radius, and cloud top height.

In both studies, ice clouds were treated relatively simple. Given that the radiative properties of ice clouds are so distinct from water clouds and that ice clouds cover about 60% of the globe, their influence warrants more investigations. The optical properties of ice clouds depend on more variables than water clouds do, including ice crystal shape, orientation, size distribution, water content, and the vertical distribution, etc. The extent of the impact by each individual variable remains largely unknown. Yet, there are currently insufficient and inaccurate measurements on most of the ice cloud variables. However, this may be improved significantly in the near future with the launch of Earth Observing System (EOS) and CloudSat satellites that can provide more information pertaining to cloud micro-physics for both water and ice clouds.

This study investigates the influence of ice clouds on the retrieval of SSRB. By conducting various sensitivity tests, it is attempted to understand the magnitude of errors due to lacking or inadequate informing on ice cloud attributes and to identify key parameters affecting the retrieval. On the basis of the sensitivity test results, parameterized corrections were derived to account for the effects of ice cloud variables.

Modeling

Radiative transfer modeling was conducted using the Fu-Liou δ -4-stream code (Fu 1996) for 429 bands at 32 vertical levels of a resolution as fine as 1 km in the troposphere. The radiative properties of atmospheric gases (water vapor, CO₂, O₃, O₂) and aerosol were calculated with MODTRAN3.5. The vertical profiles of aerosol concentration vary according to atmospheric visibility, season, and aerosol type (e.g., rural, urban, maritime, and fog type for the 0 km to 2 km layer). A set of surface spectral albedos were adopted from Clouds and Earth's Radiant Energy System/Surface and Atmospheric Radiation Budget (CERES/SARB) and adjusted for solar zenith angle (SZA). The optical properties (extinction coefficient, asymmetry factor, and single scattering albedo) of ice clouds are functions of ice particle shape and size distribution. Three crystal shapes (hexagonal column, plate, and polycrystals) are considered. The former two are often observed in ice clouds, and the optical characteristics of polycrystals are considered to be representative for bulk ice crystals (Macke et al. 1998). The generalised effective radius (D_{ge}) proposed by Fu (1996) is used to describe crystal size. The optical properties (asymmetry factor and single scattering albedo) of the three types of ice crystals are calculated with a ray-tracing method (Macke et al. 1998). They are averaged for 28 individual size distributions provided by Fu (1996). For each size distribution, phase function and single scattering albedo are computed together with its D_{ge} . Mean asymmetry factors (\bar{g}) and single scattering albedos ($\bar{\omega}$) are obtained for the 28 particle size spectra, which are fitted as functions of D_{ge} for various wavelength bins. Cloud top and bottom heights are model variables and multi-layered clouds are included.

Sensitivity Studies

Cloud Particle Effective Size and Cloud Top Height

Figure 1 illustrates the sensitivities of the intercept and slope of the relationship between SSRB (F_{abs}) and the reflected flux at TOA (F_{ref}) to ice crystal effective size D_{ge} (20 μ m to 100 μ m) and cloud top height (11 km to 8 km). The lines are fitted by regression from 136 cloudy cases and one clear-sky reference case for each SZA. From Figure 1, the slope is more sensitive to these parameters than the intercept. The slope is considerably smaller under ice cloudy conditions than under clear ones for large and medium SZAs. For small SZAs, the slope is particularly sensitive to D_{ge} with a maximum difference of 20% for the range of D_{ge} under study, which may result in the same magnitude of discrepancy in the retrieval of SSRB. Therefore, errors in the estimation of SSRB due to inadequate knowledge on cloud top height and cloud particle size increase as SZA decreases. Both the intercept and slope are more sensitive to cloud particle effective size D_{ge} than to cloud top height.

Cloud Vertical Structure

Due to gravitational sedimentation of crystals in ice clouds, the mean size of ice crystals generally decreases with height. Heymsfield et al. (1998) reported that the mean crystal sizes were tens of microns at the cloud top, 150 μ m to 200 μ m in the mid-cloud region, and maximum mean crystal sizes of about 600 μ m near the cloud bottom. Such a vertical structure in cirrus clouds exerts different effects on SSRB and TOA albedo (R_{ref}) from those of water clouds. Small crystals near cloud top reflect more solar energy (and thus less SSRB reaches at the surface) than a cloud of uniform particle size does.

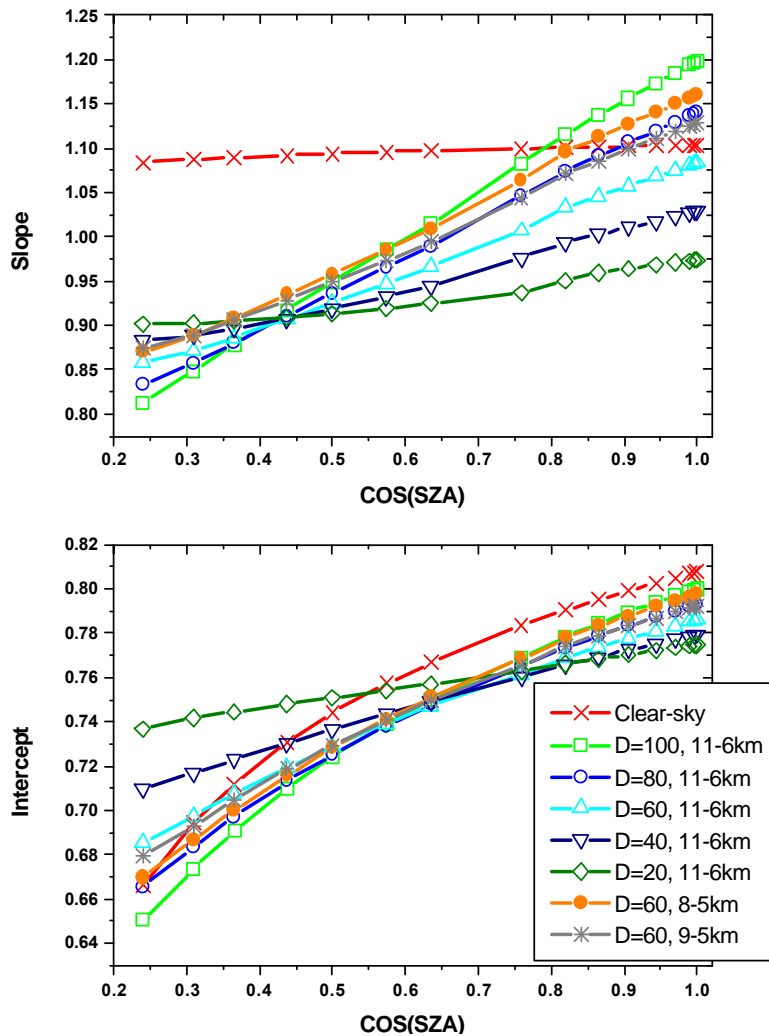


Figure 1. Intercept and slope of the F_{abs} vs. F_{ref} relationship as a function of cosine of SZA for various particle effective size (as D) and cloud top heights.

Figure 2 shows five different vertical profiles of D_{ge} with the same vertically averaged D_{ge} of $60 \mu\text{m}$ (Figure 2a) and the linear relationships between SSRB and TOA reflected flux corresponding to the five cases (Figure 2b). The differences in the relationship for the case with small crystals at the cloud top are considerably large, especially in terms of the intercept. For a given R_{ref} , discrepancy in R_{abs} (SSRB normalised by TOA incident solar irradiance) is around 0.05.

Ice clouds are often situated above water clouds. Radiative transfer in multi-layered clouds is different from that in a single-layered cloud. Satellite observation is more sensitive to the upper-most ice cloud than the water clouds below. Our model simulations suggested that errors in SSRB retrieval are about 20 Wm^{-2} if a multi-layered cloud system is treated as a single-layered ice cloud for $\text{SZA} = 60^\circ$. The error is less than that incurred by treating the ice cloud as part of the water cloud below. It varies with differences between the ice and water clouds in their particle effective size, top height, and cloud phase.

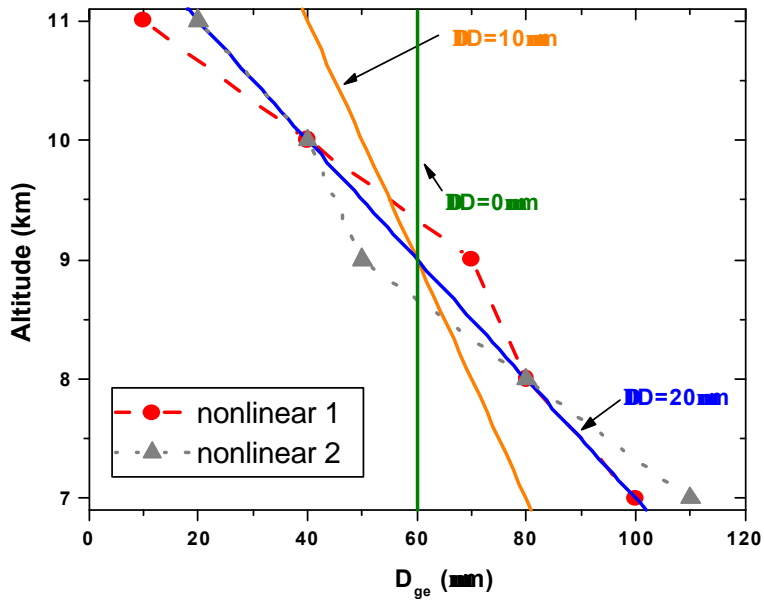


Figure 2a. Five idealised vertical profiles of ice crystal generalised effective size D_{ge} , with the same vertically averaged D_{ge} of 60 μm . ΔD : decreasing rate in crystal effective size D_{ge} ($\mu\text{m}/\text{km}$).

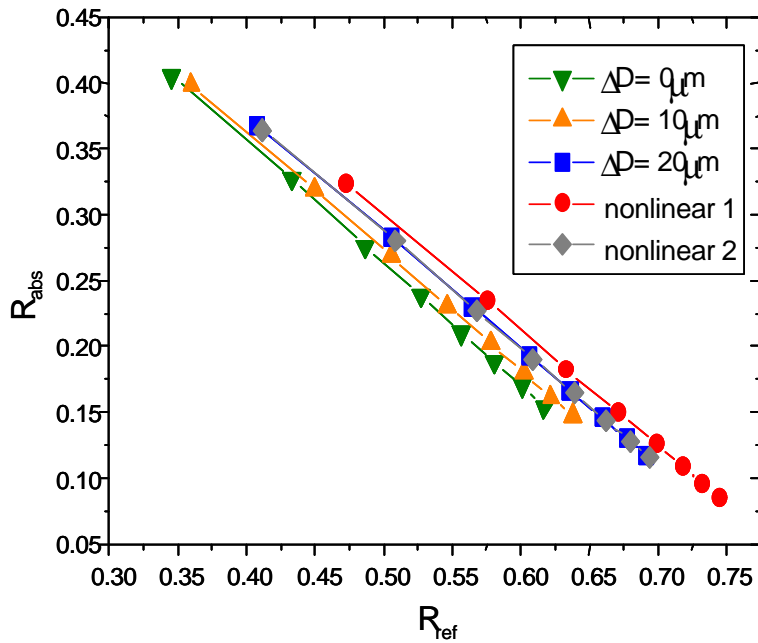


Figure 2b. Sensitivity of the linear relationship to D_{ge} vertical profile for the cases shown in Figure 2a.

Ice Crystal Shape

The non-sphericity of ice crystals influences the solar radiative properties of ice clouds. To examine the sensitivities of SSRB and its retrieval to ice crystal shape, three crystal shapes: hexagonal column, plate, and polycrystals, are taken into consideration. The sensitivities of SSRB retrieved from F_{ref} (or R_{ref}) are shown in Figure 3, in which the difference in SSRB (ΔF_{abs}) is relative to Macke's column-shaped crystals. The differences in SSRB retrieved for three ice crystal shapes are small. This means that SSRB retrieved from F_{ref} is not sensitive to ice crystal shape, despite the uncertainties in the optical properties of the non-spherical ice crystals. Therefore, ice crystal shape, one of the most difficult microphysical parameters to measure, is less influential in the SSRB retrieval.

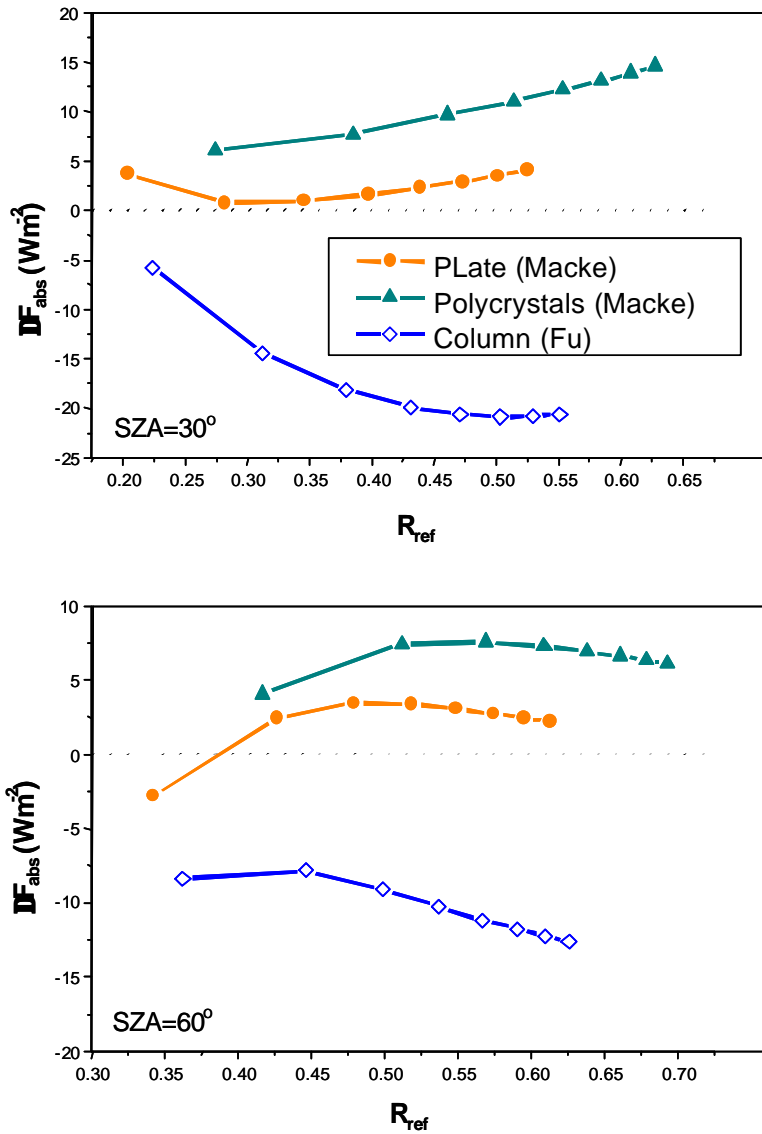


Figure 3. Difference in the retrieval of SSRB (ΔF_{abs}) between column ice crystals and other crystal shapes.

Parameterization for Ice Cloudy Sky

The effects of ice clouds are parameterized in the linear relationship between R_{abs} and R_{ref} based on the framework of Li et al. (1993). Correction terms are introduced to both the intercept and slope that are functions of SZA (μ), total column water vapour (p), crystal effective size (D_{ge}), and cloud top height (Z_t), which are sensitive variables to affect the relationship.

$$\begin{aligned} R_{\text{abs}} &= \alpha_0 + \alpha_{\text{icl}} - (\beta_0 + \beta_{\text{icl}})R_{\text{ref}} \\ R_{\text{abs}} &= \alpha_0 + \alpha_{\text{icl}} - (\beta_0 + \beta_{\text{icl}})R_{\text{ref}} \end{aligned} \quad (1)$$

$$\begin{aligned} \alpha_{\text{icl}} &= \Delta\alpha_d - \Delta\alpha_z - \Delta\alpha_v \\ \beta_{\text{icl}} &= \Delta\beta_d + \Delta\beta_z + \Delta\beta_v \end{aligned} \quad (2)$$

Where α_0 and β_0 denote clear-sky intercept and slope; α_{icl} and β_{icl} are the corrections to the intercept and slope that are given in Table 1 derived from model calculations for a large ensemble of cloudy-sky cases.

Figure 4 shows the probability of errors in the retrieval of SSRB estimated with the corrections, in comparison with those derived using the clear-sky algorithm only. Sixty water vapour profiles were employed that vary with cloud top and bottom heights, and air temperature profile, for mid-latitude summer (MLS), TRO, and mid-latitude winter (MLW) model atmospheres. Cloud top (bottom) height ranges from 14 km to 6 km (from 13 km to 2 km). Cloud particle effective size ranges from 10 μm to 130 μm . Eleven SZAs range from 8° to 76°. The cases with $D_{\text{ge}} < 40 \mu\text{m}$ and $\text{IWC} > 0.03 \text{ gm}^{-3}$ are

Table 1. The terms in the parameterization for cloudy-sky (Equation 2).	
Terms	Parameterization
Da_d	$A_1 + A_2 m + A_3 m^{2.5} + A_4 e^m$ <p>where</p> $A_1 = 3.974 \cdot 10^{-4} + 2.1781 \cdot 10^{-9} D_{\text{ge}} - (0.1387 - 0.00317 D_{\text{ge}}) / (1 - 0.02546 D_{\text{ge}} + 0.000419 D_{\text{ge}}^2)$ $A_2 = (0.1156 - 0.26 \cdot 10^{-5} D_{\text{ge}}^2) / (1 + 0.000166 D_{\text{ge}}^2 + 6.6658 \cdot 10^{-8} D_{\text{ge}}^4)$ $A_3 = -0.03157 + 0.00058 D_{\text{ge}}^2 - 1.7117 \cdot 10^{-5} D_{\text{ge}}^{2.5} + 2.77 \cdot 10^{-7} D_{\text{ge}}^3$ $A_4 = -0.1872 + 0.000472 D_{\text{ge}}^2 - 7.614 \cdot 10^{-5} D_{\text{ge}}^{2.5} + 3.18 \cdot 10^{-6} D_{\text{ge}}^3$
Db_d	$-0.16862 - 0.05361 m - 0.00218 D_{\text{ge}} + 0.04011 m^2 + 1.88541 \cdot 10^{-6} D_{\text{ge}}^2 + 0.0048 m D_{\text{ge}}$
Da_z	$\frac{0.00182 + 3.7045 \cdot 10^{-4} m - 2.6323 \cdot 10^{-4} m^2 - 8.1743 \cdot 10^{-4} \ln(Z_t)}{1 - 0.01803 m - 0.93955 \ln(Z_t) + 0.20939 (\ln(Z_t))^2}$
Db_z	$0.016529 - 0.00163 Z_t^{2.5} + 3.68857 \cdot 10^{-4} Z_t^3 + 1.95822 e^{-Z_t}$
Da_v	$0.04921 - 0.08217 m - 0.07588 p^{-1} + 5.9372 \cdot 10^{-3} m^2 - 0.03459 p^{-2} + 0.1555 m p^{-1}$
Db_v	$0.0585 - 0.01972 \sqrt{p} \ln(p) - 0.1292 \frac{\ln(p)}{p^2}$

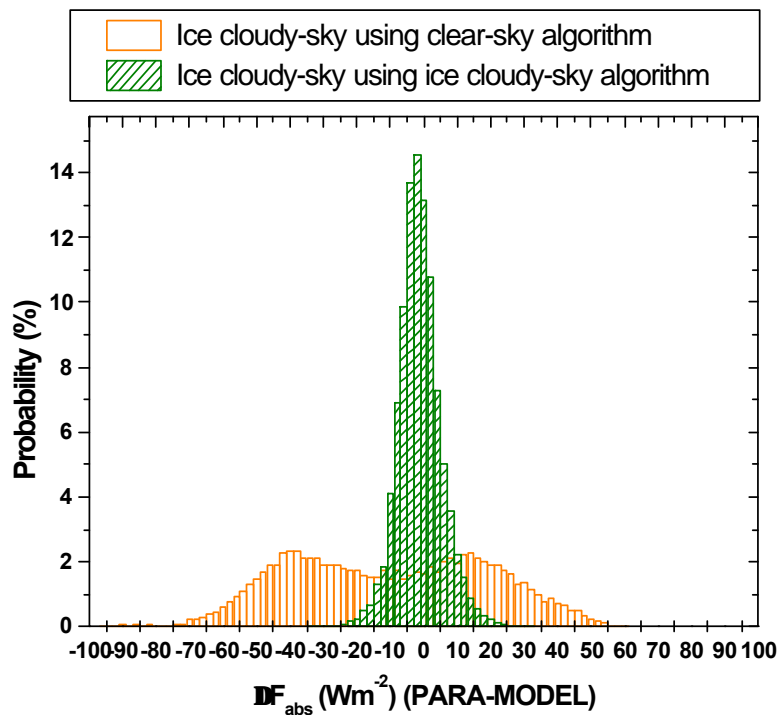


Figure 4. The probability of errors in F_{abs} (parameterization [PARA] minus model simulations [MODEL]) for various cloudy-sky atmospheric cases, in which D_{ge} varies from $10 \mu\text{m}$ to $130 \mu\text{m}$, cloud top height from 6 km up to 14 km, cloud bottom height from 2 km to 13 km, SZA from 8° to 76° ; and the calculation is for grasslands and 66 water vapour profiles in MLS, TRO, and MLW atmospheres. The probability of errors due to the use of the clear-sky retrieval algorithm is also given for the same cases.

excluded. The probability of errors within $\pm 10 \text{ Wm}^{-2}$ is 91%, computed for over 19,000 cases. In contrast, the probability of the same error range resulting from the use of the original clear-sky algorithm is only 19%. Applying these corrections to water cloud cases lead to a probability of 55% for errors within $\pm 10 \text{ Wm}^{-2}$. This suggests that different correction should be applied for water clouds.

Summary

- The retrieval of SSRB under cloudy conditions is sensitive to cloud water phase, particle size, cloud top height.
- The relationship between SSRB and TOA reflected flux depends on the vertical profile of ice crystal size, in particular, on the size of crystals near the cloud top.
- Ice crystal particle shape has a relatively minor impact on the relationship.
- The effects of ice cloud variables on the retrieval of SSRB are parameterized which can considerably reduce the estimation uncertainty.

Acknowledgement

The study was supported by the U.S. Department of Energy (DOE) under Atmospheric Radiation Measurement (ARM) grants DE-FG02-97ER2361.

References

Fu, Q., 1996: An accurate parameterization of the solar radiative properties of cirrus clouds for climate models. *J. Climate*, **9**, 2058-2082.

Hemysfield, A. J., L. M. Miloshevich, G. M. McFarquhar, and S. M. Aulenbach, 1998: Nonspherical ice particles in cirrus clouds. AMS light scattering conference, New York.

Li, Z., H. G. Leighton, K. Masuda, and T. Takashima, 1993: Estimation of SW flux absorbed at the surface from TOA reflected flux. *J. Climate*, **6**, 318-330.

Macke, A., P. N. Francis, G. M. McFarquhar, and S. Kinne, 1998: The role of ice particle shapes and size distributions in the single scattering properties of cirrus clouds. *J. Atmos. Sci.*, **55**, 2874-2883.

Masuda, K., H. G. Leighton, and Z. Li, 1995: A new parameterization for the determination of solar flux absorbed at the surface from satellite measurements. *J. Climate*, **8**, 1615-1629.